Journal of
Applied Crystallography
ISSN 0021-8898

Received 16 August 2006
Accepted 8 January 2007

Small-angle X-ray scattering measurements of expanded fluid Se in the semiconductor–metal transition region using synchrotron radiation

Masanori Inui,[a]* Kazuhiro Matsuda,[b] Kozaburo Tamura,[b] Kohei Satoh,[b] Atsushi Sobajima[b] and Hirotoshi Tada[b]

[a]Graduate School of Integrated Arts and Sciences, Hiroshima University, Higashi-Hiroshima, 739-8521, Japan, and [b]Graduate School of Engineering, Kyoto University, Kyoto, 606-8501, Japan. Correspondence e-mail: inui@mls.ias.hiroshima-u.ac.jp

Small-angle X-ray scattering measurements for expanded fluid Se were carried out up to the semiconductor–metal transition region at high temperature and high pressure. A broad peak appears in the small-angle X-ray scattering profiles in the temperature range 1273 to 1773 K at 60 MPa, which suggests a correlation length of 50 Å. We fitted the patterns using a model function proposed by Teubner & Strey [*J. Chem. Phys.* (1987), **87**, 3195–3200] and obtained two characteristic lengths, the domain size of the dense and rare regions, and the correlation length concerning their boundary. The present results suggest peculiar density fluctuations accompanying the SC-M transition in fluid Se consisting of polymeric molecules.

1. Introduction

Liquid Se, a typical liquid element semiconductor, consists of linear polymeric molecules where the atoms are covalently bonded. It undergoes a semiconductor–metal (SC-M) transition with increasing temperature at high pressure. The first indication of the SC-M transition in fluid Se was obtained from d.c. conductivity data (Hoshino *et al.*, 1976). Fig. 1 shows the phase diagram of fluid Se as a function of pressure and temperature. The thin broken line denotes the saturated vapor pressure curve and the open circle is the liquid–vapor critical point. The critical temperature, pressure and density of fluid Se are T_C = 1888 K, P_C = 38.5 MPa and ρ_C = 1.85 g cm^{-3}, respectively (Hosokawa *et al.*, 1997). The thin solid lines in Fig. 1 denote the contour of the d.c. conductivity. Many experimental results (Tamura, 1996, and references therein) show that the SC-M transition occurs gradually near the contour of 30 Ω^{-1} cm^{-1}, as indicated by a bold broken line in Fig. 1. The characteristic features of the SC-M transition in fluid Se are as follows: First, the metallic state in fluid Se appears with volume expansion, despite the fact that expanded metals usually transform to insulators. In fact, with further volume expansion, the metallic fluid Se transforms into an insulating vapor. Second, the average chain length becomes shorter as the volume expands, as investigated by nuclear magnetic resonance measurements (Warren & Dupree, 1980). This fact suggests that the SC-M transition is strongly correlated with structural instability of the chain molecule.

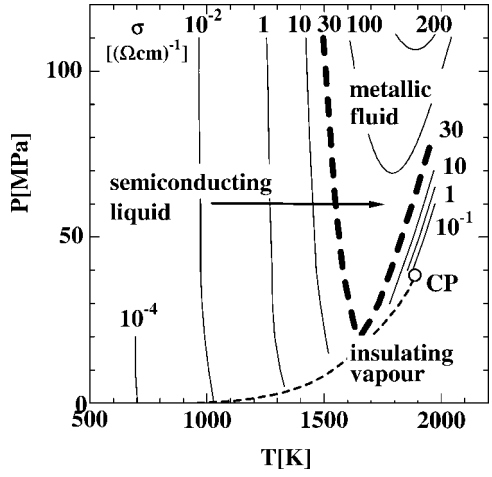

Figure 1
Phase diagram of fluid Se as a function of pressure and temperature.

To understand the mechanism of the SC-M transition, information on atomic configuration is crucial. Wide-angle X-ray scattering (WAXS) measurements for expanded fluid Se were first carried out up to the metallic region by Tamura & Hosokawa (1992). They found that the twofold coordinated structure in the semiconducting region is largely preserved in the metallic state while the covalent bond becomes slightly shorter during the SC-M transition. These results were confirmed again by new data obtained from WAXS using synchrotron radiation (Tamura & Inui, 2001). X-ray absorption fine structure spectroscopy has also been used to study expanded fluid Se (Soldo *et al.*, 1998), allowing the change of the local structure during the SC-M transition to be observed. Recently, the local structure and the electronic density of states in expanded fluid Se were investigated by *ab initio* molecular dynamics simulations and details of the local structure during the SC-M transition have been clarified (Shimojo *et al.*, 1998; Kirchhoff *et al.*, 1998; Raty *et al.*, 1999).

Although experiments and simulations have shown the change of local structure during the SC-M transition in fluid Se, the relation between the long-range structure and the SC-M transition is still not known. Small-angle X-ray scattering (SAXS) patterns of fluid Se near the critical point have been reported (Tamura & Inui, 2001; Coulet *et al.*, 2003) but few data have been reported in the SC-M transition region so far (Inui *et al.*, 1996; Coulet *et al.*, 2003). In our case, this is because the large background from a Be window of the high-pressure vessel obscured the weak signal of fluid Se in the SC-M transition

region (Tamura & Inui, 2001). We have developed a second high-pressure vessel equipped with a large diamond window for scattered X-rays and have succeeded in suppressing the background very much. Now we can obtain reliable SAXS patterns of expanded fluid Se in the SC-M transition region that can be used to discuss the long-range structure, such as density fluctuations. In this article, we present new SAXS data for expanded fluid Se and report density fluctuations in the SC-M transition in fluid Se.

2. Experimental

SAXS measurements were carried out using synchrotron radiation on the BL04B2 beamline at SPring-8. Details of the BL04B2 beamline are given in the literature (Isshiki *et al.*, 2001). For SAXS measurements, monochromated 38 keV X-rays were incident on the sample and the scattered X-rays were detected with an imaging plate. The imaging plate was typically exposed for 20 min per pattern. An ionization chamber was put in front of the imaging plate before and after a SAXS measurement to measure the intensity of transmitted X-rays for an absorption correction.

The experiments at high temperature and high pressure were performed using an internally heated high-pressure vessel made of super-high-tension steel. The apparatus permits measurements to be made up to 2000 K and 196 MPa. High pressures were created using compressed He gas (99.9999%). The vessel has transparent synthetic diamond windows of the highest quality, which are 3 and 6.3 mm in diameter for the incident and scattered X-rays, respectively. The modulus of the scattering vector, Q, is defined as $Q = (4\pi/\lambda)\sin\theta$, where 2θ and λ are the scattering angle and the X-ray wavelength, respectively. The observable Q range is usually 0.04 to 0.4 Å^{-1}, but the minimum value of Q, $Q_{\rm min}$, in the present experiments was slightly worse (0.07 Å^{-1}) due to a rapid increase of the background intensity at 0.05 Å^{-1}. Parasitic scattering may accidentally have occurred due to stains on the diamond windows, because the patterns for fluid Se were measured straight after SAXS measurements of fluid Rb, and a tight beamtime schedule did not allow enough time to clean the windows between the two experiments.

The Se sample (99.999%) was contained in a poly-crystal sapphire cell for the SAXS measurements. The sample thickness was 0.5 mm. No parasitic scattering was observed from the cell, even at high temperature. The background from an empty cell was measured at the same high temperature and high pressure. The scattering intensity from compressed He gas was measured at 300 K and at several pressures up to 60 MPa to estimate the absolute scattering intensity. As the statistics of SAXS patterns are much better when using synchrotron radiation than Mo K_α radiation from an old rotating anode, the absolute scale becomes more reliable. We believe that the present error for the absolute scale is at most 10%.

3. Results and discussion

We measured SAXS patterns at 60 MPa in the temperature range 873 to 1873 K across the SC-M transition around 30 Ω^{-1} cm^{-1} as indicated by the arrow in Fig. 1. SAXS intensities, $I(Q)$, of fluid Se at several temperatures and typical background data after a transmission correction are plotted in Fig. 2. For fluid Se, $I(Q)$ increases with decreasing Q but has a broad shoulder around 0.12 Å^{-1}. We estimated the absolute scale of $I(Q)$ for fluid Se using that of compressed He gas. When the coherent scattering intensity, $I^{\rm coh}(Q)$, of fluid Se is obtained from the observed $I(Q)$ after subtracting the background, we can deduce the structure factor, $S(Q)$, from the equation $I^{\rm coh}(Q) = Nf(Q)^2S(Q)$, where N and $f(Q)$ are the number of atoms and the atomic form factor of Se, respectively. Fig. 3 shows $S(Q)$ values for fluid Se at 60 MPa and at the temperatures indicated in the figure. In the semiconducting region, less than 1273 K, $S(Q)$ values for the observed Q range were small. At 1273 K, the $S(Q)$ values start to increase and a broad peak at 0.13 Å^{-1} appears. With increasing temperature, the maximum around 0.13 Å^{-1} becomes large and the peak position shifts slightly to smaller Q values, while the $S(Q)$ values at $Q_{\rm min}$ also increase, along with an increase in the $S(0)$ values deduced from the thermodynamic quantities (Hosokawa *et al.*, 1997). Coulet *et al.* (2003) have measured SAXS patterns of fluid Se in the same temperature and pressure range and concluded that the density contrast between the semiconducting and metallic domains was too small to detect using SAXS. Their SAXS intensity profiles show a slight enhancement at smaller Q values in the SC-M transition region,

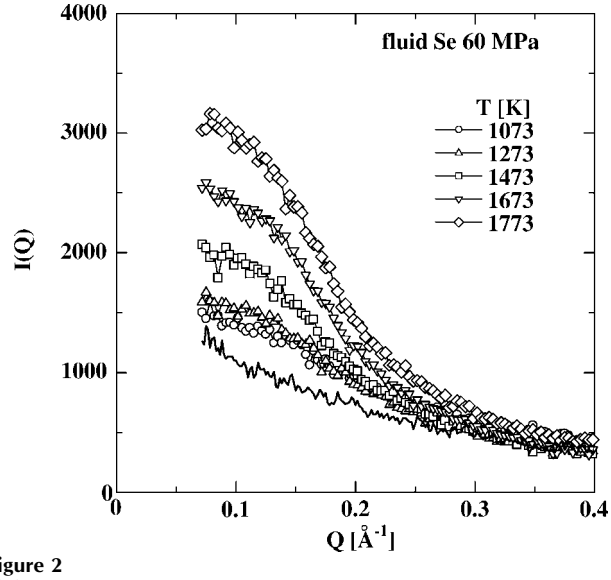

Figure 2
$I(Q)$ values for fluid Se. A typical background is shown by a solid line.

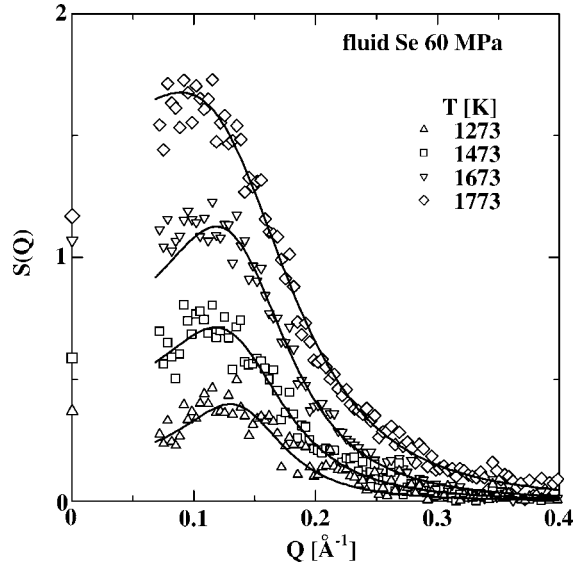

Figure 3
Structure factors $S(Q)$ of fluid Se. The symbols denote the experimental data and the solid lines denote the best fits with the model function. $S(0$ values obtained from thermodynamic data are represented by the symbols on the ordinate.

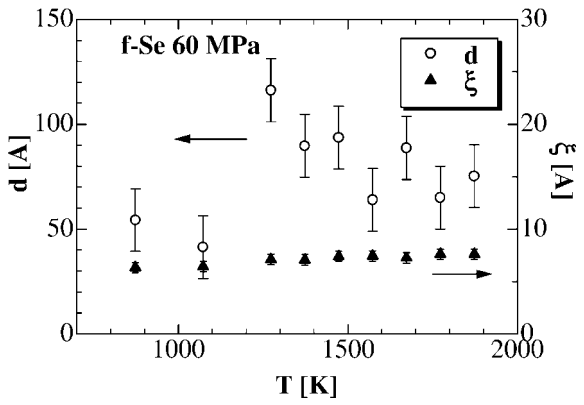

Figure 4
The domain size, d, and the correlation length, ξ, as a function of temperature.

although they described the patterns as flat. Since they did not deduce $S(Q)$ from their SAXS patterns, direct comparison of our results with theirs is difficult. However, we think that they observed a sign of the density contrast accompanying the SC-M transition, while the broad peak at 0.13 Å^{-1} was not observable in their data.

The profile of the present $S(Q)$ values in the SC-M transition region does not follow the Ornstein–Zernike scattering law, while $S(Q)$ values near the critical point do. We tried to fit the $S(Q)$ values using a model function, $I^{\rm coh}(Q) \simeq (a_2 + c_1Q^2 + c_2Q^4)^{-1}$, proposed by Teubner & Strey (1987). This model function provides a single broad maximum for negative c_1 before decaying according to Q^{-4}, and its Fourier transform is related to the correlation function in real space, $\gamma(r)$ (Debye & Bueche, 1949), by $\gamma(r) = (d/2\pi r)\exp(-r/\xi)\times \sin(2\pi r/d)$, where r, d and ξ are the distance, the length of the periodicity, and the correlation length, respectively. We carried out a least-square fitting of the data using the model function and obtained values for the parameters a_2, c_1 and c_2. The optimized $S(Q)$ values are indicated by solid lines in Fig. 3.

We calculated d and ξ from the optimized a_2, c_1 and c_2 values using the equations in the literature (Teubner & Strey, 1987). d and ξ are plotted as a function of temperature in Fig. 4. We now consider the meaning of the lengths d and ξ in fluid Se. While the d values are quite scattered, ξ remains almost constant at 7 Å. This distance corresponds to the fourth or fifth nearest-neighbor distance in a disordered chain and about twice the interchain distance. On the other hand, d in the semiconducting region is about 50 Å and it seems to increase to 70–100 Å in the SC-M transition and metallic regions. A simulation (Shimojo *et al.*, 1998) shows that when the metallic nature of fluid Se is enhanced, the average chain length becomes short, and breaking and branching of the chain actively occurs. At the same time, the macroscopic volume slightly contracts. Thus d of about 100 Å must correspond to the size of dense and rare domains in density fluctuations. Since fluid Se is not a simple monatomic fluid but consists of short polymeric molecules in the SC-M transition region, the boundary region between the dense and rare regions may form a third region, having a correlation length of about 7 Å, as presented by ξ in this model.

4. Summary

We have measured SAXS patterns of fluid Se in the SC-M transition region at high temperature and high pressure. After background subtraction, the observed patterns were transformed to $S(Q)$ values using the scaling factor obtained from the SAXS intensity of compressed He gas. The $S(Q)$ values in the SC-M transition region in fluid Se have a broad peak at 0.13 Å^{-1}, suggesting the existence of dense and rare domains with a size of 50 Å. The boundary between the domains may form a third domain with a correlation length of 7 Å.

The authors are grateful to Professor K. Hoshino, Professor F. Shimojo, Professor S. Hosokawa, Dr Y. Ohishi and Dr S. Kohara for valuable discussions. The authors would also like to thank Mr M. Muranaka for his valuable work on machining. This work is supported by Grant-in-Aids for Scientific Research from the Ministry of Education, Science and Culture of Japan. The synchrotron-radiation experiments were performed at SPring-8 with the approval of the Japan Synchrotron Radiation Research Institute (JASRI) (Proposal No. 2004B0069-ND2a-np).

References

Coulet, M.-V., Simonet, V., Calzavara, Y., Testemale, D., Hazemann, J.-L., Raoux, D., Bley, F. & Simon, J.-P. (2003). *J. Chem. Phys.* **118**, 11235–11238.
Debye, P. & Bueche, A. M. (1949). *J. Appl. Phys.* **20**, 518–525.
Hoshino, H., Schmutzler, R. W. & Hensel, F. (1976). *Ber. Bunsenges. Phys. Chem.* **80**, 27–31.
Hosokawa, S., Kuboi, T. & Tamura, K. (1997). *Ber. Bunsenges. Phys. Chem.* **101**, 120–127.
Inui, M., Noda, T., Tamura, K. & Li, C. (1996). *J. Phys. Condens. Matter*, **8**, 9347–9352.
Isshiki, M., Ohishi, Y., Goto, S., Takeshita, K. & Ishikawa, T. (2001). *Nucl. Inst. Methods Phys. Res. A*, **467–468**, 663–666.
Kirchhoff, F., Kresse, G. & Gillan, M. J. (1998). *Phys. Rev. B*, **57**, 10482–10495.
Raty, J. Y., Saùl, A., Gasperd, J. P. & Bichara, C. (1999). *Phys. Rev. B*, **60**, 2441–2448.
Shimojo, F., Hoshino, K., Watabe, M. & Zempo, Y. (1998). *J. Phys. Condens. Matter*, **10**, 1199–1210.
Soldo, Y., Hazemann, J.-L., Aberdam, D., Inui, M., Tamura, K., Raoux, D., Pernot, E., Jal, J.-F. & Dupuy-Philon, J. (1998). *Phys. Rev. B*, **57**, 258–268.
Tamura, K. (1996). *J. Non-Cryst. Solids*, **205–207**, 239–246.
Tamura, K. & Hosokawa, S. (1992). *Ber. Busenges. Phys. Chem.* **96**, 681–688.
Tamura, K. & Inui, M. (2001). *J. Phys. Condens. Matter*, **13**, R337–R368.
Teubner, M. & Strey, R. (1987). *J. Chem. Phys.* **87**, 3195–3200.
Warren, W. W. & Dupree, R. (1980). *Phys. Rev. B*, **22**, 2257–2275.